

APPLICATIONS OF INFRARED THERMOGRAPHY

IN NONDESTRUCTIVE EVALUATION

Xavier Maldague

Electrical and Computing Engineering Dept., Université Laval,
Quebec City (Quebec), G1K 7P4, Canada
phone: (418) 656-2962, fax: (418) 656-3594, email: maldagx@gel.ulaval.ca

1. Introduction

This text is intended as a brief introduction to infrared thermography (IRT) for nondestructive evaluation (NDE) including discussions about applications, and future trends. More detailed and complete information about IRT for NDE can be found in [1,2,3] among other references.

In order to present an up-to-date panorama of current activities, a compilation in tabular form from last two editions of major conferences in the field is presented: *Thermosense* in North America and *QIRT* (Quantitative Infrared Thermography) in Europe.

2. Active and passive thermography for NDE

IRT for NDE is aimed at the discovery of subsurface features (such as subsurface thermal properties, presence of subsurface anomalies/defects), thanks to relevant temperature differences observed on the surface with an infrared (IR) camera. Figure 1 illustrates the general concept.

IRT is deployed along two schemes, *passive* and *active*. The *passive* scheme tests materials and structures which are naturally at different (often higher) temperature than ambient while in the case of the *active* scheme, an external stimulus is necessary to induce relevant thermal contrasts (which are not available otherwise, e.g. specimen at uniform temperature prior to testing).

3. Advantages and difficulties of IR thermography

Each NDE technique has its own strengths and weaknesses. In the case of thermography these are as follows:

- fast inspection rate;
- no contact;
- security (no harmful radiation involved, however high power external stimulation - such as

powerful flashes - requires screens during flashes);

- results relatively easy to interpret (image format);
- wide range of applications (sometimes unique NDE tool).

On the other hand, difficulties are as follow:

- difficulty to deposit uniformly a large amount of energy in short period of time over a large surface (for the pulsed active approach, see below);
- effects of thermal losses (convective, radiative, conductive) perturbing thermal contrasts;
- cost of the equipment (IR camera, thermal stimulation units for active thermography);
- capability to detect only entities (subsurface defects) resulting in a measurable change of thermal properties;
- ability to inspect a limited thickness of material under the surface (thermography is a 'boundary' technique);
- emissivity problems (section 4.1).

4. Theory

4.1 *Radiometry, emissivity and temperature measurement*

As discussed in the previous section, IRT as its name implies, is a non contact sensing method concerned with the measurement of radiated electromagnetic energy. The energy emitted by a surface at a given temperature is called the spectral radiance and is defined by the Planck's law [1, p. 25]. An IR camera is in fact a spectral radiometer measuring this energy and proper calibration (based on the Planck's law) allows to retrieve the temperature distribution on the surface of interest. Polynomials are commonly used to convert gray level values g obtained from the IR camera into temperature T [1, chap. 3]. An example of such equation is (bottom camera, Figure 2 below):

$$T(^{\circ}\text{C}) = -13.4 + 0.05g - 1.6 \times 10^{-5}g^2 + 2.2 \times 10^{-9}g^3. \quad (1)$$

Such equation is valid in a given span of temperature providing an high emissivity surface is observed within a close distance (see below).

For NDE applications, involved distances are small and the atmosphere is, in most of the cases,

considered transparent in the spectral bands of interest where absorption is limited: 3-5 μm (short waves or SW) or in the 8-12 μm (long waves or LW). See ref [2], chap. 3 for a complete discussion on IR detectors and cameras.

An important problem of such IR measurement is the emissivity ϵ (strictly speaking ϵ should refer to 'emittance' however to avoid possibility of confusion with the radiant energy flux that also uses 'emittance', 'emissivity' is used in this text). Emissivity is a surface property that specifies the ability of that surface to emit energy, values of ϵ are between 0 (for a perfect reflector) to 1 (for a perfect emitter, called a 'blackbody.') Emissivity has dependences with surface orientation, temperature, wavelengths. A surface having a low emissivity acts as a mirror and makes measurements difficult since spurious radiations emitted by warm neighboring bodies perturb readings through reflections. Various techniques are deployed to solve low or uneven emissivity problems. Among them, covering the inspected surface with a high emissivity flat paint ($\epsilon \sim 0.9$) is the most common one for imaging applications [1, p. 139].

4.2 Heat transfer considerations

When a quantitative analysis is necessary, some pre-analysis of the experiment is convenient. This is called the "direct problem" which consists to "predict" the thermal behavior of the surface under consideration either analytically (for simple situations) or through heat transfer modeling by finite elements or finite differences. Dedicated program packages are available from various vendors (e.g. COSMOS/M, Thermo.Heat 3D). Such pre-analysis is useful to establish the limits of the effectiveness of the procedure, to consider different defect geometries and determine their detectability without the expense of making and testing the corresponding specimens.

Once experimental results are available, the "inverse problem" refers to the ability to quantitatively characterize properties of a given "hot spot." This can take place with for instance abaci, family of curves or empirical equations established from the direct modeling [5].

5. Passive thermography

The first law of thermodynamics concerns the principle of energy conservation and states that an important quantity of heat is released by any (industrial) process consuming energy because of the law of entropy. Temperature is thus an essential parameter to measure in order to assess proper operation. Common applications of the passive scheme in NDE are for buildings, components and

processes, maintenance, medicine and properties evaluation. Table 1 lists recent reported applications. In these applications, abnormal temperature profiles indicate a potential problem relevant to detect. In passive thermography, the key words is the temperature difference with respect to the surrounding, often referred to as the 'delta-T' or the "hot spot." A delta-T of 1 to 2 °C is generally found suspicious while a 4°C value is a strong evidence of abnormal behavior. In most of the applications, passive thermography is rather qualitative since the goal is simply to pinpoint anomalies of the type go/no-go. These applications are generally based on empirical rules applied by experienced personal (know-how of the trade).

Some investigations are however more sophisticated and provide quantitative measurements. In these cases, a direct thermal modeling (section 4.2) is necessary. For instance in a reported application, such approach is proposed in the case of needles used to sew fabrics in the automobile industry (seat cushions and backs, airbags, etc.) [4]. In this study a model is developed to simulate the needle heating during high speed sewing. This help to better understand needle heating which is further confirmed by experimental measurements on the plant floor, Figure 2. Heating (up to 100-300°C) comes from friction between the needle and the fabric and increases at high speed causing serious problems such as worn or broken thread, fabric scorching, tempering and weakening needle (sewing is performed in between 1000 to 3000 rpm). Understanding mechanisms of needle heating allows to take actions to optimize sewing operations through for instance needle redesign and needle cooling with significant economic and quality benefits due to the million of sewed products daily.

6. Active thermography

The active scheme has numerous applications in NDE. Moreover since characteristics of the required external stimulus are known somehow such as for instance the time t_0 when it is applied, quantitative characterization becomes possible. In this text, the accent is on the active scheme. Various modes of thermal stimulation are available. Briefly covered will be: pulsed thermography, step-heating, lockin thermography and vibrothermography.

6.1 Pulsed thermography

Basically, pulsed thermography (PT) consists to briefly heat the specimen and then record the temperature decay curve. Qualitatively, the phenomenon is as follow. The temperature of the

material changes rapidly after the initial thermal pulse because the thermal front propagates, by diffusion, under the surface and also because of radiation and convection losses. The presence of a defect reduces the diffusion rate so that when observing the surface temperature, defects appear as areas of different temperatures with respect to surrounding sound areas once the thermal front has reached them. Consequently, deeper defects will be observed later and with a reduced contrast. In fact, the observation time t is function (in a first approximation) of the squared of the depth z and the loss of thermal contrast c is proportional to the cube of the depth:

$$t \sim \frac{z^2}{\alpha} \quad \text{and} \quad c \sim \frac{1}{z^3} \quad (2)$$

where α is the thermal diffusivity of the material.

These relations indicate two limitations of the IRT: observable defects will generally be shallow and the thermal contrasts will be weak. An empirical rule of thumb says that *the radius of the smallest detectable defect should be at least one to two times larger than its depth under the surface*. This rule is valid for homogeneous isotropic material. In case of anisotropy it is more constrained.

Various deployments are possible: • point inspection (example: laser or focused light beam heating), • line inspection (example: heating with line lamps, heated wire, line of air jets (cool or hot), scanning laser), • surface inspection (example: heating using lamps, flash lamps, scanning laser); either in reflection (thermal source and detector located on the same side of the inspected component) or in transmission (heating source and detector located on each side of the component). Figure 3 shows a picture of a typical set-up, in reflection.

Interestingly, if the temperature of the part to inspect is already higher than ambient temperature due to the manufacturing process for instance, it might be convenient to make use of a cold thermal source such as a line of air jets. Obviously, a thermal front propagates the same way whether being hot or cold: what is important is the temperature differential between the thermal source and the specimen. Another advantage of a cold thermal source is that it does not induce spurious thermal reflections into the IR camera as in the case of a hot thermal source.

As an illustration of PT, Figure 4 shows IR images (also called thermograms) recorded on a CFRP (carbon fiber reinforced plastic) plate with a simulated defect (5 mm diameter hole, 2 mm under

the front surface). Heating is performed in reflection using high power lamps with back reflector (for a total of 6 kW of electric energy, pulse duration was set to 200 ms, similar set-up as for Figure 3). Knowledge of the evolution of thermal contrast above the defect in conjunction with equations derived from inverse heat transfer modeling (section 4.2) allows to retrieve defect parameters such as depth, diameter, thermal resistance [1, chap. 6]. A common definition of the thermal contrast C is:

$$C(t) = \frac{T_i(t) - T_i(t_0)}{T_s(t) - T_s(t_0)} \quad (3)$$

where T is the temperature signal, t is the time variable, subscripts i and s refer respectively to over a suspected defective location (that is in fact any pixel in the image) and over sound areas respectively. C is computed with respect to before heating temperature distribution at time t_0 (to suppress the adverse contributions from the surrounding environment) and normalized by the behavior of a sound area so that a unit value is obtained over a non defect area. Such kind of analysis is common in the aerospace industry where composite materials such as CFRP are widely used. Other common applications of the active PT scheme are in quantitative subsurface defect assessment (cracks, delaminations, impact damages, disbondings, moisture), thermophysical property evaluation; in all kind of industries (aerospace, metal, buildings, etc.). Table 2 lists recent reported applications.

6.2 Step heating (long pulse)

Contrary to PT scheme for which the temperature decay is of interest (after the heat pulse), here the increase of surface temperature is monitored during the application of a step heating (SH) pulse ('long pulse'). Variations of surface temperature with time are related to specimen features. This technique is sometimes referred to as time-resolved infrared radiometry or TRIR. TRIR finds applications such as for coating thickness evaluation (including multi-layered coatings). More details about this technique can be found in [6,7]. For instance, an empirical relationship provides the coating thickness L [6]:

$$t_c = \frac{0.36L^2}{\alpha}, \quad (4)$$

once the thermal transit time t_c is determined, α is the thermal diffusivity. In such experiments,

the coating specimen is heated and the temperature is plotted versus the square root of time, Figure 5. The thermal transit time is observed when the curve begins to depart from the semi-infinite case (which is a straight line in such plots). The experimental set-up is similar to the one depicted on Figure 1, but for the heating which is constant during the measurement, for instance using a laser (e.g. argon/ion laser).

Other common applications of the SH thermography scheme are listed in Table 3.

6.3 Lockin thermography

Lockin thermography (or LT) is based on thermal waves generated inside the specimen under study in the permanent regime [8,9]. Here, the specimen is submitted to a sine-modulation heating at a frequency ω which introduces highly attenuated and dispersive thermal waves of frequency ω inside the material (in a close to the surface region). The resulting oscillating temperature field in the stationary regime is remotely recorded through its thermal infrared emission with the infrared camera. The lockin terminology refer to the necessity to monitor the exact time dependence between the recorded temperature signal and the reference signal (*i.e.* the sine-modulation heating). This can be done with a lock-in amplifier in a point by point laser heating or with a computer in full-field deployment. The experimental set-up is similar to the one depicted on Figure 1 and 3, but for the heating which is permanent and of sine-modulation nature (either laser point heating or full-field have been reported with commercial equipment available).

In LT, phase and magnitude images become available through simple manipulations of thermograms recorded in the permanent regime. A thermogram is a mapping of the emitted thermal infrared power while a phase image is related to the propagation time and a modulation image is related to the thermal diffusivity. A strong point of LT for NDE is the phase image which is relatively independent of local optical surface features (such as non-uniform heating).

The depth range of magnitude image is roughly given by the thermal diffusion length μ expressed by:

$$\mu = \sqrt{2k/\omega\rho c} \quad (5)$$

with thermal conductivity k , density ρ , specific heat c and modulation frequency ω . In the case of phase images the depth range is about twice larger [9]. Eq. (5) indicates that higher modulation

frequencies will restrict the analysis in a near surface region while lower frequencies will allow to probe deeper under the surface. This is illustrated on Figure 6, in the case of a CFRP specimen of the kind used in the aerospace industry.

One potential difficulty of LT is related to the acquisition time which should cover at least one modulation cycle: 0.12 Hz requires at least 8 s, 0.06 Hz requires at least 16.6 s and 0.03 Hz requires at least 33.3 s (parameters of Figure 6). These values should be compared with time values for straight thermograms in the pulsed scheme of Figure 4 where for a similar defect: thermal contrast appears as early as 7 s after the heating pulse. Moreover, if a wrong heating frequency ω is chosen, a defect might be missed (Figure 6 at $\omega = 0.12$ or 0.03 Hz).

On the other hand, thanks to the relative insensitivity of phase images to non-uniform heating and also to the ease modulated heating is deployed, large areas ($\sim 2 \text{ m}^2$) can be inspected in one experiment provided the spatial resolution of the infrared camera allows detection of the smallest defects of interest [10].

Another field of application for LT is the characterization of electromagnetic fields, especially their interaction with metallic structures. In this application, the structure of interest (such as a thin film introduced in a horn antenna) is coated with a magnetic paint sensitive to the electromagnetic field or with an electrically conductive coating. The heating of these coatings can be related to the electromagnetic field and surface currents. In the steady state regime the high thermal conductivity of the structure distorts the coating heating which does not witness accurately the electromagnetic field and surface currents. However, in the modulated regime, if the modulation frequency is sufficiently high to have a diffusion length μ smaller than the coating thickness (eq. 5), the modulated heating will not be blurred by the thermal diffusion into the metallic substrate. For this application, the magnitude image is of interest since it is proportional to the intensity of the source and thus to the electromagnetic field intensity [11]. The phase image which is related to the heat transfer phenomena as described previously is not interesting for this application.

Other common applications of the active LT scheme are reported in Table 4.

6.4 Vibrothermography

Vibrothermography (VT) is a technique where under the effect of mechanical vibrations induced

externally to the structure, direct conversion from mechanical to thermal energy occurs and heat is released by friction precisely at locations where defects such as cracks and delaminations are located [12, 13]. By changing (increasing or decreasing) the mechanical excitation frequency, local thermal gradients appear or disappear at specific resonance frequency. Direct modeling allows to determine such suitable excitation frequencies. For instance in a given study, a 28 x 13 cm CFRP beam is attached to a piezoelectric shaker from one side and significative thermal patterns from the simulated delamination embedded in the specimen (of size 10 x 7 mm) appear only with mechanical excitation around 13.5 KHz [12], Figure 7.

An alternative deployment of lockin thermography scheme is related to VT. In that case a mechanical excitation of the specimen is obtained thanks to an ultrasonic transducer (shaker) attached to the specimen (conversely, the specimen can be partly immersed into an ultrasonic bath): the high frequency ultrasonic signal (typ. 40 kHz) is modulated with a low frequency signal which creates a thermal wave of desired wavelength as in conventional LT while the high frequency acts as a carrier delivering heating energy right inside the specimen [14, 15]. This technique called loss-angle heating at ultrasonic frequencies is reported to detect deeper and smaller defects while the selective heating allows a better discrimination among detected defects. Typical applications are for detection of corrosion, vertical cracks and delaminations.

VT most significant advantages are: detection of flaws hardly visible by other IR thermography schemes (such as in the case of closed cracks), its ability to inspect large structural areas *in situ*. On the other hand, the required mechanical loading might be sometimes difficult to achieve.

Other recent reported applications of the VT scheme are listed in Table 5.

7. Which scheme to choose from?

Interestingly, we saw that different approaches can be used for similar problems. Examples of CFRP inspection were shown in pulsed, lockin and vibrothermography schemes (Figures 4,6,7). Then a question arises: which one to select? This is a difficult question and the answer depends really of what ones is looking for.

For instance if suspected defects are closed cracks, VT might provide a solution. If defects are at known depth (for instance in the case of large bonded laminates), LT at optimized modulation frequency (eq. 5) would be a good choice. On the other hand, if defect depth is not known, PT might

be the answer combined , if object size is large, with a robotic arm to move the inspection head (camera and flashes, Figure 2).

Moreover, passive and active thermography are not as clear-cut choices as it might first appear. For instance moisture investigation in buildings can be assessed in the passive scheme (thanks to solar heating for instance) or provoked in a pulsed active scheme through blowing of warm/cold air from inside the suspected wall (Table 1 and 2).

Although thermal modeling (section 4.2) could also help answering this question, up to now trial and errors seems to be the rule. This might change in the near future thanks to the recent initiative lead by the QIRT Working Group through Round-Robin tests of blind specimens that go through several research groups for IRT NDE tests by several of the methods discussed in this chapter. Before full results become available, the question of the best scheme to choose from for a given application is still on the research agenda.

8. Trends

Looking at the evolution of IRT in NDE, three directions are clearly seen in hardware, software and applications.

8.1 Hardware

Dedicated hardware for IRT aimed at NDE is improving. Thanks to progresses in microelectronics, focal plane arrays (FPA) with quantum (cooled) detectors are now available with direct digital interface (14 bits is now common while 6-7 bits was the rule in the late eighties), low noise (often smaller than 20 mK while 0.1 K was an achievements only a few years ago), high spatial resolution (up to 512 x 512 pixels), greater uniformity (> 99.5 %) while they are no longer tied to video standards of 25 or 30 Hz. For instance model SBF 136 from Lockheed Martin (Goleta, USA) has a frame rate of 30 000 Hz allowing to capture very fast thermal transients.

Prior to these advances, the basic IR camera consisted in a single detector piece with an electro-mechanical scanning system: noise was high and performance is limited. Although high performance IR cameras such as the SBF 136 are still reserved for high-end applications due to their cost (> 100 K\$ US), most of the IR sensors are following such trends.

In low-end applications a new comer is the array of uncooled micro-bolometers which took the market as a storm in the mid 90s. A bolometer is a thermal detector, that is a detector which is

sensitive to the heating of its own surface (e.g. the electrical resistivity changes with temperature and such changes are monitored). Advanced microelectronics allows, through machining, to stack thousands of these tiny detectors on a silicon substrate along with dedicated electronics. Contrary to quantum detectors which need to be cooled down to cryogenic temperatures to operate (e.g. at liquid nitrogen temperature, $-192\text{ }^{\circ}\text{C}$, 77 K), room temperature is sufficient for bolometers. The main limitation of micro-bolometer-based IR cameras is the low frame rate (due to the thermal inertia of the detectors that have to be heated themselves (quantum detectors operate faster through photon detection)).

Computer hardware with enhanced capabilities add to such improvements. For instance, huge amount of data (complete thermogram sequences in PT) can be acquired, calibrated, processed and stored in real-time (the days of the video tape recorder with limited bandwidth is now gone). Digital signal processor (DSP) boards which are autonomous boards fitting in to a PC offer tremendous amount of computational power (e.g. the TMS320C62xx DSP from Texas Instruments delivers 400 millions of additions/multiplications per second). Harnessing such processing open new horizons.

8.2 Software

Thanks to number-crunching (portable) computers (and boards), dedicated software for IRT offers new possibilities (unrealistic before due to lengthy processing time).

For instance the use of transforms such as the Fourier transform applied to the whole thermogram sequence in PT. In this respect, the recently introduced Pulse Phase Thermography (PPT) processing scheme [16]. PPT is a novel technique which combines somehow advantages of both PT and LT. In PPT deployment, the specimen is pulse-heated as in PT and the mix of frequencies of the thermal waves launched into the specimen is unscrambled by performing the Fourier transform of the temperature decay on a pixel by pixel basis. This enables computation of phase images as in LT. The process is as follow, for each pixel (i,j). The temporal decay $f(x)$ is extracted from the image sequence (where x is the index in the image sequence). Next, from $f(x)$, the discrete Fourier transform $F(\omega)$ is computed (ω being the frequency variable). Finally, from the real $R(\omega)$ and imaginary $I(\omega)$ components of $F(\omega)$, the phase ϕ is computed using the well known formula $\phi(\omega) = \text{atan}\{I(\omega)/R(\omega)\}$. In PPT as in LT, it is possible to explore the various frequencies ω . However an important point to remember is that in PPT the analysis is performed in the transient

mode with many frequencies available from a single experiment, while in LT the signal is recorded in the stationary mode with one frequency per experiment. Figure 8 show examples of PPT images very similar to the ones shown in Figure 6 obtained in straight LT scheme.

Interestingly, such frequency per frequency analysis removes the blurring observed on Figure 4 (similar specimen). Such blurring is due to the mix of thermal waves of many different frequencies in the time-domain thermograms because pulsed heating corresponds in fact to the launching of thermal waves of many different frequencies (the Fourier transform $F[.]$ of an ideal Dirac pulse $\delta(t)$ contains all frequencies: $F[\delta(t)] = 1$).

As said previously, automatic diagnosis is an area where developments are to be expected. Algorithms specially dedicated to such tasks are thus in demand. Among them, artificial intelligence techniques such as the use of neural networks are popular in IRT due to the large amount of data to handle (e.g. thermogram sequence in PT).

A neural network (NN) is a set of small processors highly interconnected together and having individually a small memorization capability they learned from information submitted to them in the first place. Generally the network is divided into layers and the parallel nature of these NN make them well suited to work on multi-parameter problems such as infrared images. Once the architecture of the NN is established (such as Perceptron, Kohonen, etc.), a training phase is necessary to configure the weights associated to individual neurons before actual deployment. More details and examples of applications can be found in [17-23].

8.3 Applications

Thanks to more sophisticated IR cameras, computer, computer accessories and processing software, new applications are emerging continuously. It is noticed by looking at Table 1 that from all these reported applications, 23 were from last conference editions and 43 from the current ones, almost a two-fold growth. Although not a scientific survey, this confirms clearly the trend: new applications are emerging for IRT applied to NDE. For instance micro-bolometer based IR camera rugged and requiring no cooling are now deployed on the plant floor for continuously monitoring industrial processes. Associated with DSP boards, alarms are raised automatically. These applications are reported for instance in the glass industry where abnormal temperature profile indicates reduced tolerance to breakage. In such applications, software monitor plant temperature

(which can vary with seasons and weather) and spurious reflections in real-time for enhanced diagnosis. Such integrated approach: IR image sensor, computer processor to interpret data and machine control interface to provide feed-back is now referred to as infrared machine vision [24].

New applications are also expected in the active scheme thanks to 'new heating deployments' such as Joule heating, lateral heating, microwave heating. For instance, in the case of microwave heating, a time-gated microwave source introduces heat into the specimen and, for homogeneous specimens, this allows detection of subsurface microwave absorbing features (such as water-filled areas, metal wires or fibers) through infrared imaging. Moreover, if the host is transparent to microwaves, the microwave source heats these features directly. In this case, a higher spatial resolution is noticed (as compared with the surface heating case) since the transit time of the thermal front is shorter and consequently the three-dimensional spreading losses (thermal wave blurring) are reduced: the thermal front has only to diffuse to the surface instead of being of a round trip nature. Quantitative information can be extracted by analyzing the time and spatial dependence of the surface temperature [25, 26].

These are only examples of what is to be expected in the near future.

9. Conclusion

In this chapter we covered briefly fundamentals of infrared thermography in nondestructive evaluation both in passive and active schemes with accent on applications. A discussion was added on future trends.

10. Acknowledgments

The supports of the Natural Sciences and Engineering Research Council of Canada and of the Fonds FCAR from Québec Province are acknowledged.

11. References

- [1] Maldague X., *Nondestructive evaluation of materials by infrared thermography*, London, Springer-Verlag, 224 p., 1993 (new revised edition, *John Wiley & Sons Pub.*, exp. in 2001).
- [2] Maldague X. ed., *Infrared Methodology and Technology*, Gordon and Breach, NY, 525 p., 1994.
- [3] Kaplan H., *Practical applications of infrared thermal sensing and imaging equipment*, SPIE vol. TT 13, 137 p., 1993.

- [4] Li. Q., Liasi E, Simon D., Du R., “Heating of industrial sewing machine needles: FEA model and verification using IR radiometry,” in *Thermosense XXI*, Proc. SPIE, R.N. Wurzbach, D.D. Burleigh eds., **3700**: 347-357, 1999.
- [5] Krapez J. C., Maldague X., Cielo P., “Thermographic NonDestructive Evaluation: Data inversion procedures, Part II: 2-D Analysis and Experimental Results,” *Research in Nondestructive Evaluation*, **3**: 101-124, 1991.
- [6] Spicer J.W.M., Kerns W.D., Aamodt L.C., Murphy J.C., “Time-resolved infrared radiometry (TRIR) of multilayer organic coatings using surface and subsurface heating” in *Thermosense XIII*, Proc. SPIE, G. S. Baird ed., **1467**: 311-321, 1991.
- [7] Spicer J.W.M., Wilson D.W., Osiander R., Thomas J., Oni B.O., “Evaluation of high thermal conductivity graphite fibers for thermal management in electronics applications,” in *Thermosense XXI*, Proc. SPIE, R.N. Wurzbach, D.D. Burleigh eds., **3700**: 40-47, 1999.
- [8] Busse G., Wu D., Karpen W., “Thermal wave imaging with phase sensitive modulated thermography,” *J. Appl. Phys.*, **71**[8]: 3962-3965, 1992.
- [9] Busse G., “Nondestructive evaluation of polymer materials,” *NDT & E Int’l*, **27**[5]: 253-262, 1994.
- [10] Wu, D., Salerno A., Malter U., Aoki R., Kochendörfer R., Kächele P.K., Woithe K., Pfister K., Busse G., “Inspection of aircraft structural components using lockin-thermography,” *QIRT-96 (Quantitative Infrared Thermography)*, Eurotherm Seminar 50, D. Balageas, G. Busse, C. Carlomagno eds., Edizioni ETS (Pisa, Italy) , pp 251-256, 1996.
- [11] Balageas D., Levesque P., “EMIR: A photothermal tool for electromagnetic phenomena characterization,” *Rev. Gén. Therm.*, **37**: 725-739, 1998.
- [12] Tenek L.H., Henneke E.G., “Flaw dynamics and vibro-thermographic thermoelastic NDE of advanced composite materials” in *Thermosense XIII*, Proc. SPIE, G. S. Baird ed., **1467**: 252-263, 1991.
- [13] Dinwiddie R.B., Blau P.J., “Time-Resolved Tribo-Thermography,” in *Thermosense XXI*, Proc. SPIE, R.N. Wurzbach, D.D. Burleigh eds., **3700**: 358-368, 1999.
- [14] Rantala J., Wu D., Busse G., “Amplitude modulated lock-in vibrothermography for NDE of polymers and composites” in *Research in NDE*, **7**: 215-228, 1996.
- [15] Salerno A., Wu D., Busse G., Rantala J., “Thermographic inspection with ultrasonic excitation” in Proc. of *Rev. Progresses in Quantitat. NDE*, D.O. Thompson, D.E. Chimenti eds., NY: Plenum press, **16A**: 345-352, 1996.
- [16] Maldague X., Marinetti S., “Pulse Phase Infrared Thermography,” *J. Appl. Phys.*, **79**[5]: 2694-2698, 1996.
- [17] Prabhu, D.R., Howell, P.A., Syed, H.I., Winfree, W.P., “Application of artificial neural networks to thermal detection of disbonds,” *Review of Progress in Quantitative NDE*, D.O.

Thompson, D.E. Chimenti eds, **11B**: 1331-13382 (Plenum Press, 1992).

- [18] Trétout H., David D., Marin J.Y., Dessendre M., “An evaluation of artificial neural networks applied to infrared thermography inspection of composite aerospace structures”, *Review of Progress in Quantitative NDE*, D.O. Thompson, D.E. Chimenti eds, **14**: 827-834, (Plenum Press, 1995).
- [19] Hagan M. T., Demuth H. B., Beale M., *Neural networks design*, PWS publishing company, 1996.
- [20] Santey M.B., Almond D. P., “An artificial neural network interpreter for transient thermography image data”, *NDT & E Int.*, **30**[5]: 291-295, 1997.
- [21] Bison P.G., Marinetti S., Manduchi G., Grinzato E., “Improvement of neural networks performances in thermal NDE,” *Advances in Signal Processing for Non Destructive Evaluations of Materials*, X. Maldague ed., American Soc. of Non Destructive Testing Press, **TONES 3**: 221-227, 1998.
- [22] Maldague X., Largouët Y., “Depth study in pulsed phase thermography using neural networks: Modeling, noise, experiments,” *Revue Générale de Thermique*, **37**[8]: 704-708, Sept. 1998.
- [23] Sarle, W.S., “Neural Network FAQ (<ftp://ftp.sas.com/pub/neural/FAQ.html>), May 1999.
- [24] Foucher B., “Infrared machine vision,” in *Thermosense XXI*, Proc. SPIE, R.N. Wurzbach, D.D. Burleigh eds., **3700**: 210-213, 1999.
- [25] d’Ambrosio G., Massa R., Migliore M.D. et al. “Microwave excitation for thermographic NDE: An experimental study and some theoretical evaluations *Materials Evaluation*, **53**[4]: 502-508, Apr. 1995.
- [26] Sakagami T., Kubo S., “Proposal of a new thermographical nondestructive testing technique using microwave heating,” in *Thermosense XXI*, Proc. SPIE, R.N. Wurzbach, D.D. Burleigh eds., **3700**: 99-103, 1999.

Figure 1 - General concept of infrared thermography aimed at nondestructive evaluation.

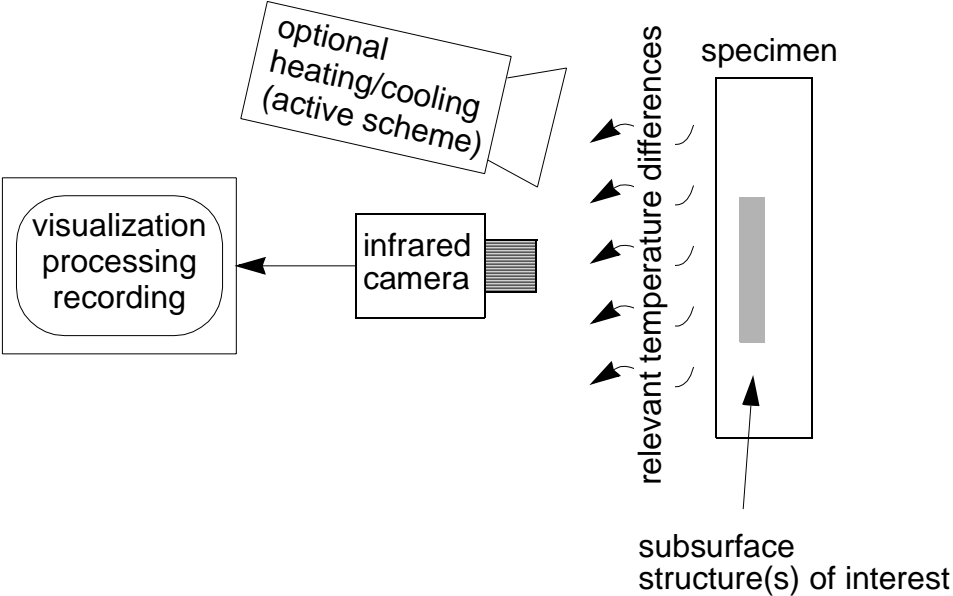


Figure 2 - Passive thermography for industrial needle heating study: (a) industrial sewing machine needle geometry, (b) simulation depicting needle temperature distribution, (c) thermogram of needle at medium speed, reproduced with permission from [4].

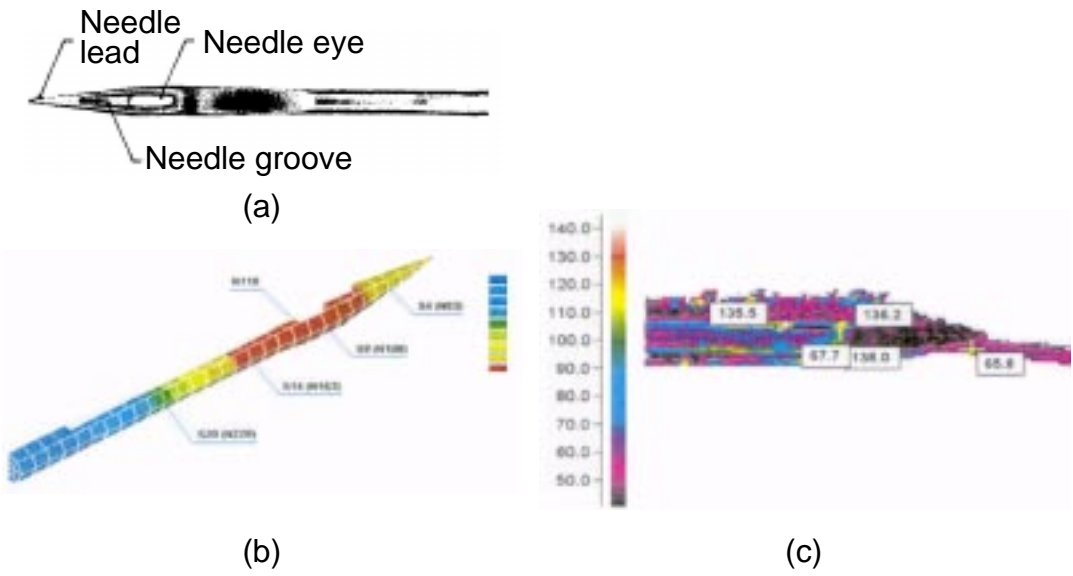


Figure 3 - Picture of an experimental set-up for active pulsed thermography, in reflection. In this case, two infrared cameras are deployed, one on top of the other for observation in both short (bottom) and long (top) wavelengths.



Figure 4 - Active pulsed thermography. Thermogram sequence recorded on a CFRP (carbon fiber reinforced plastic) plate with a simulated defect (5 mm diam. hole, 2 mm under the front surface). Progression of the thermal contrast is clearly seen (maximum thermal contrast occurs at 20.64 s). Flashes are fired at $t = 0$ s.

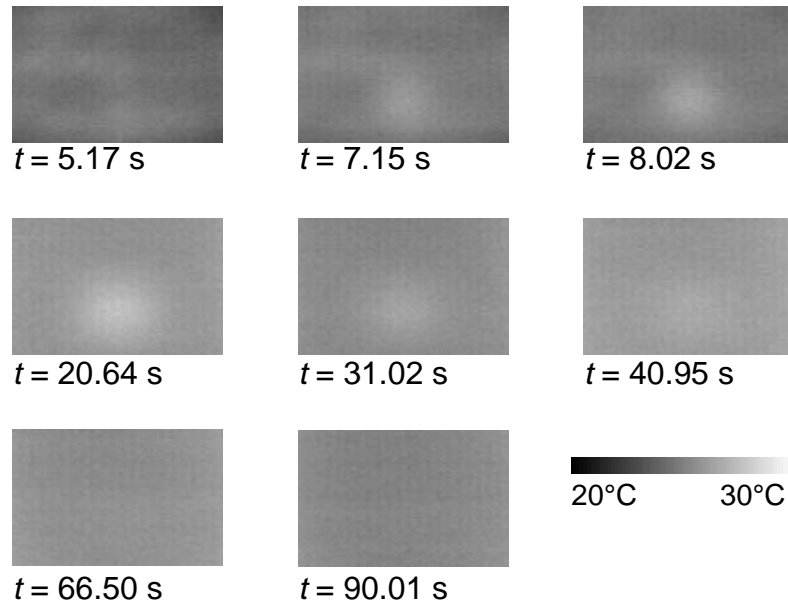
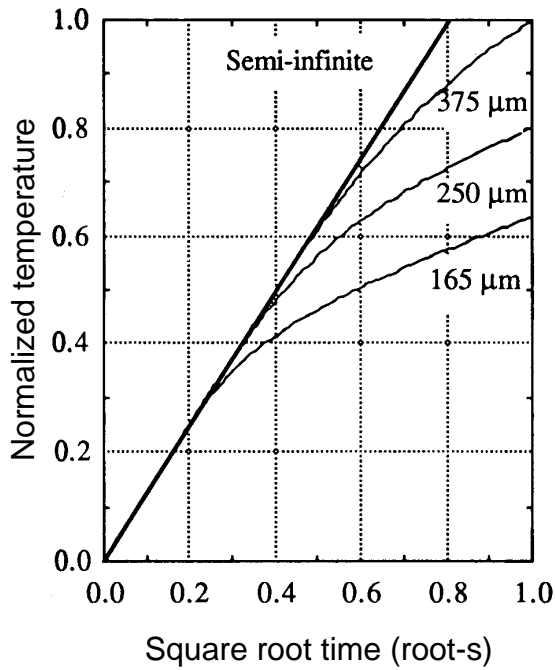
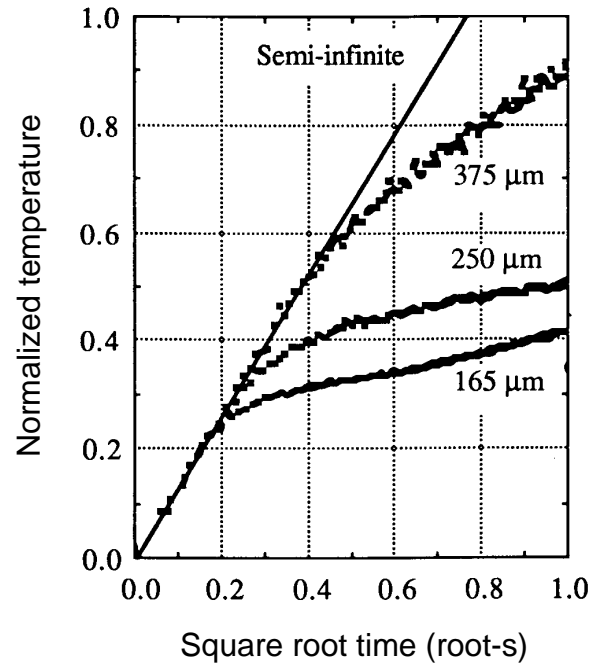


Figure 5 - Active step-heating thermography. Temporal evolution of normalized temperature for a series of zirconia coatings of different thicknesses for a step heating pulse of 1 s: (a) theoretical calculation, (b) experimental results, reproduced with permission from [6].



(a)



(b)

Figure 6 - Active lockin thermography. Phase images recorded over a CFRP (carbon fiber reinforced plastic) 4 mm-thick plate with simulated defects (teflon implants of 20 mm diameter, 2 mm (bottom-right) and 3 mm (top-left) under the front surface). Effect of the heating frequency ω is clearly seen (three experiments at different frequencies ω).

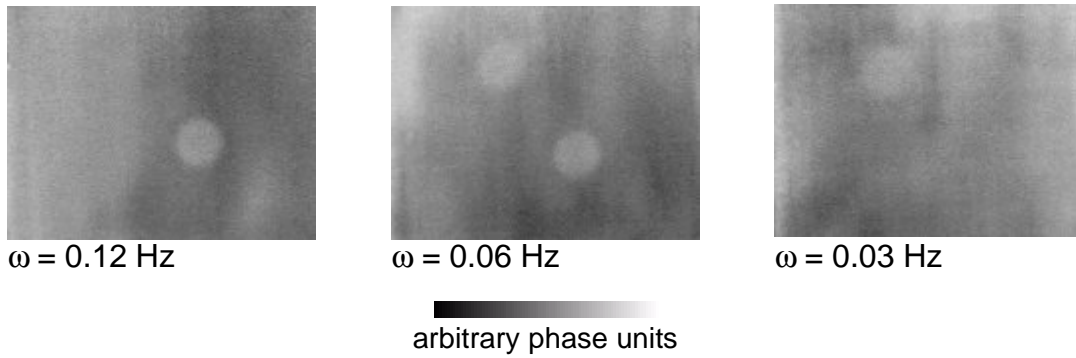


Figure 7 - Active vibrothermography: (a) finite element discretization of damaged (90/0/90) beam, (b) normalized energy along center of delamination nodes as function of frequency (in kHz) and (c) thermogram at 13.5 KHz, showing heat generated by the excited flaw, adapted and reproduced with permission from [12].

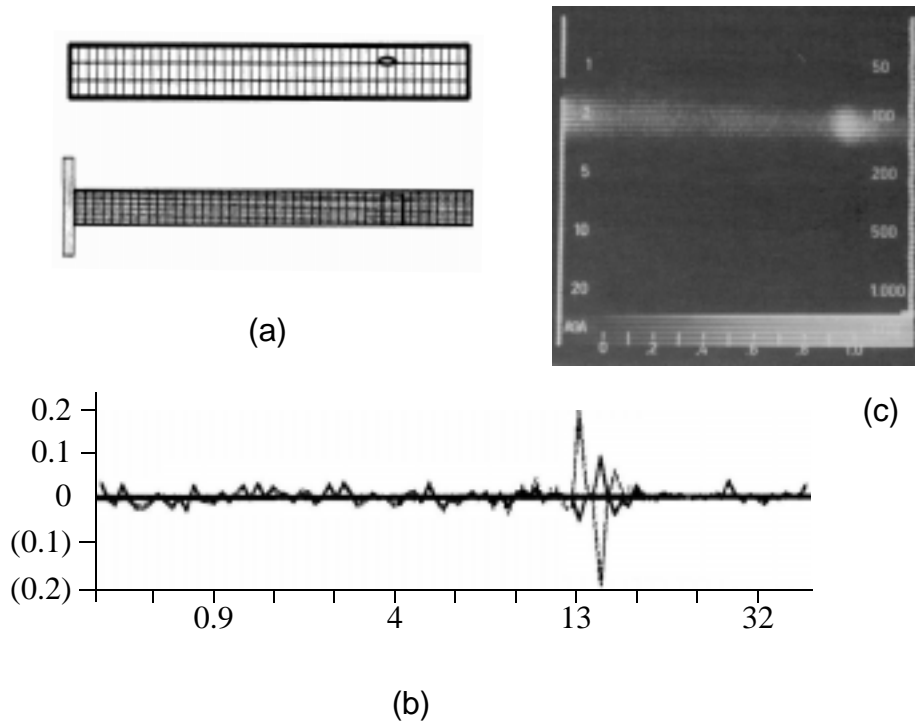
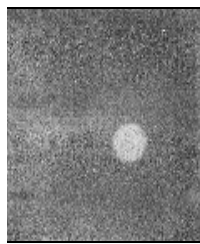
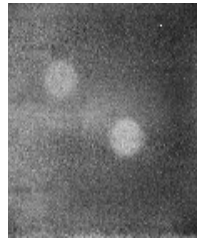


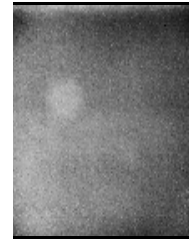
Figure 8 - Active pulsed thermography. Use of Fourier transform in pulsed phase thermography approach. Same specimen as Figure 6 (a single experiment was sufficient to provide results at three different frequencies ω).




$\omega = 0.188$ Hz



$\omega = 0.063$ Hz



$\omega = 0.020$ Hz

 arbitrary phase units